ACI STRUCTURAL JOURNAL TECHNICAL PAPER

Title No. 119-S72

Shear Hinge Model for Analysis of Reinforced Concrete Columns

by Amir Reza Tabkhi Wayghan and Vahid Sadeghian

One of the most computationally efficient and practical modeling methods for nonlinear analysis of reinforced concrete (RC) structures is the lumped plasticity approach. Despite its popularity, the application of the lumped plasticity method to analysis of shear-critical RC structures has been limited mainly because of the lack of a robust shear hinge model. This paper presents a rational shear hinge model for nonlinear analysis of RC columns that is capable of capturing advanced mechanisms in RC and axial-flexure-shear interaction effects. The model is developed based on fundamental equations of equilibrium and compatibility in conjunction with well-recognized constitutive material models, enabling its application to a wide range of structures. The accuracy and application range of the model are assessed by analyzing a large number of shear-critical RC columns with various design parameters and comparing the results against those obtained from experimental tests and detailed finite element analyses. The effectiveness of the proposed model for system-level analysis is also shown by modeling a multi-story frame structure.

Keywords: lumped plasticity; nonlinear analysis; reinforced concrete columns; shear behavior.

INTRODUCTION

Performance and safety assessment of reinforced concrete (RC) structures using nonlinear analysis methods is constantly growing among researchers and engineers. Existing nonlinear analysis methods can be classified into three main groups: detailed finite element (FE) modeling, fiber-based analysis method, and lumped plasticity analysis method. The most comprehensive and accurate analysis method is FE modeling, which is typically used for evaluating the response of individual structural members (beams, columns, joints, and so on). This analysis method enables detailed assessment of the behavior by dividing structural members into a large number of two-dimensional (2-D) or three-dimensional (3-D) elements and computing nonlinear stresses and strains for each element. However, FE analysis is computationally time-consuming and requires significant modeling effort, making it almost impractical to be used for analysis of large structural systems. The fiber-based and lumped plasticity modeling methods are more suitable for system-level analysis of structures. By using one-dimensional (1-D) frame-type elements and a set of simplifying assumptions, these methods significantly improve the computational performance of the analysis. The fiber-based analysis method (also known as the distributed plasticity method) uses a set of fibers, often formulated based on the assumption that plane sections remain plane, to calculate nonlinear stresses and strains along the cross section. In recent years, some researchers introduced novel multi-scale modeling methods[1,2] where the critical parts of the structure are modeled using FE analysis tools and the rest of the structure is modeled with a fiber-based analysis software. Despite being accurate and computationally efficient, application of these methods requires a strong knowledge of computer modeling.

A more computationally efficient analysis method suitable for use in engineering offices is the lumped plasticity approach. With this analysis method, nonlinearity effects are assumed to be concentrated at specific points (that is, plastic hinges), which are expected to be critical regions of the structure, while linear elastic behavior is assumed for the rest of the structure. The accuracy of the lumped plasticity analysis method is directly related to the ability of plastic hinges to capture nonlinearity effects. The number of plastic hinge models developed for nonlinear analysis of shear-critical RC columns is limited. A summary of the shear hinge models available in the literature is provided by Tabkhi and Sadeghian.[3] Most of the existing models either have a limited application range,[4,5] require extensive calibration,[5] neglect important mechanisms such as axial-flexural-shear interaction effects,[5] or require using an analysis tool for calculation of the shear force-shear deformation response.[5,6] Also, none of the existing models account for second-order material effects in cracked reinforced concrete (for example, aggregate interlock and compression softening in concrete), which are known to have significant effect on the shear behavior.[4-6]

Recently, the authors proposed a comprehensive rational plastic hinge model[3] for nonlinear analysis of shear-critical RC beams formulated based on the Modified Compression Field Theory (MCFT),[7] a well-recognized smeared rotating crack model for computing the response of RC structures. This paper extends the formulation of the recently developed plastic hinge model to the nonlinear analysis of shear-critical RC columns. This requires taking into account the effects of axial load on the shear force-shear displacement response at different structural damage states (concrete cracking, reinforcement yielding, and so on), while ensuring that the compatibility and equilibrium requirements are satisfied. The model is verified against experimental tests of shear-critical RC columns and its application range is evaluated through an extensive parametric study. Lastly, both shear plastic hinge models developed by the authors for analysis of beams and columns are used to demonstrate the effectiveness of the

ACI Structural Journal, V. 119, No. 3, May 2022.

MS No. S-2021-356.R1, doi: 10.14359/51734499, received November 29, 2021, and reviewed under Institute publication policies.

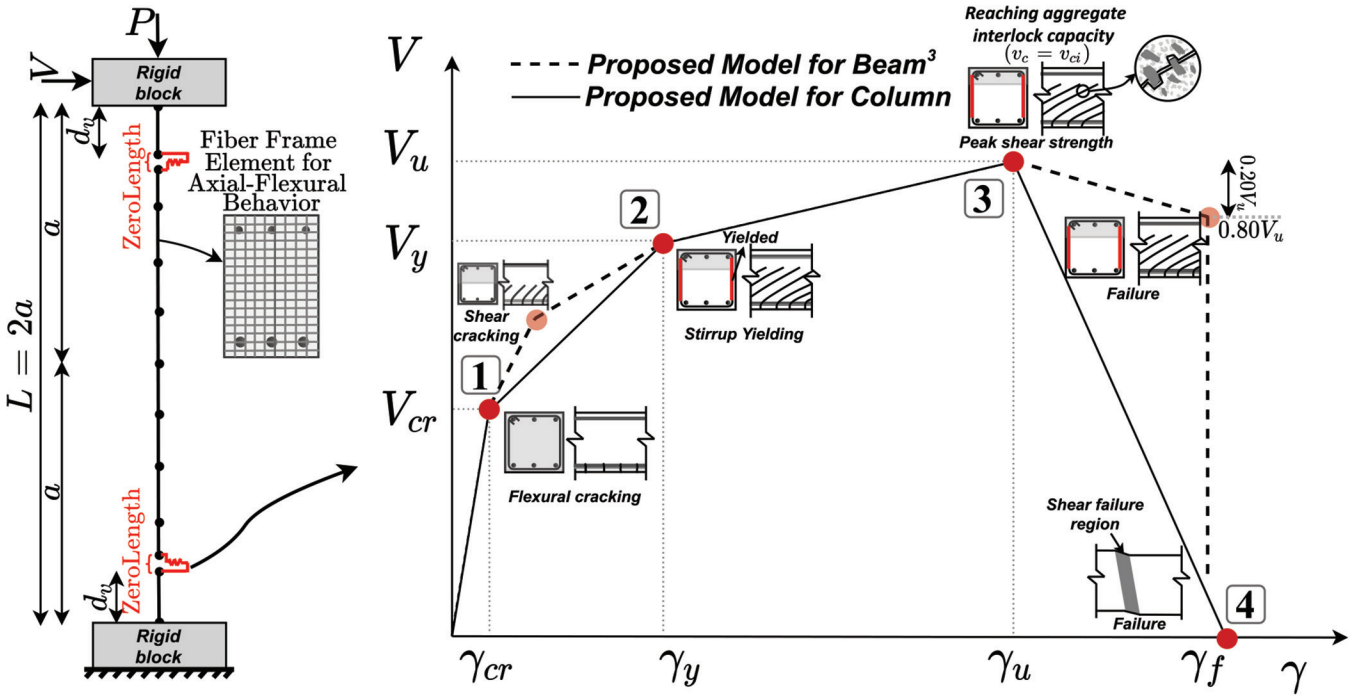

Fig. 1—Schematic shear force-shear strain curves for shear hinge models proposed for beams and columns.

proposed modeling approach for system-level performance assessment of a multi-story frame.

RESEARCH SIGNIFICANCE

The simplicity and computational efficiency of the lumped plasticity approach make it an ideal nonlinear analysis method for safety and performance assessment of RC structures at the system level. However, because of the lack of a robust shear hinge model, the application of the lumped plasticity method has been mostly limited to computing the flexural response of RC structures. This paper presents a comprehensive shear hinge model for nonlinear analysis of RC columns that improves the application of the lumped plasticity analysis approach to shear-critical structures. By considering nonlinearity effects due to shear at the system-level, the proposed modeling approach will enhance the safety assessment of existing structures and contribute to the design of high-performance complex structural systems.

MODEL FORMULATION

Similar to the shear hinge model developed for beams by the authors,[3] a multilinear curve for shear force versus shear strain relationship is proposed for columns, as shown in Fig. 1. Four key points on this curve are considered, representing the various stages of the shear response: concrete cracking, yielding of transverse reinforcement, ultimate shear strength, and shear failure. As shown in Fig. 1, the key points considered for the beam and column model have two major differences. First, the shear cracking point in the beam model is removed from the column model. In the beam model, this point was defined as when diagonal shear cracks approximately reach the middepth of the section. Because of the presence of axial compressive load in columns, however, the tensile zone in the section becomes relatively small, and the shear cracks typically do not reach the middepth prior to yielding of the transverse reinforcement (refer to Fig. 1). This change also makes the model more simplified without affecting its accuracy.

The second change is in the definition of the post-peak response. For beams, the failure point was defined as a point where there was a 20% reduction in the peak shear strength, which was then followed by an abrupt decline in the response. This definition was considered acceptable as there has not been much research done on the post-peak response of shear-critical beams. In comparison, there are a few studies dedicated to the failure point of shear-critical columns. The model proposed by Elwood and Moehle[8] developed based on the shear-friction theory, and the model proposed by Tran and Li[9] formulated based on the energy concept are two examples of these studies. The post-peak response of shear-critical columns will be discussed in more detail in the "Failure Point" section.

In general, there are two main differences between the characteristic behavior of RC beams and columns that need to be investigated. First, the presence of axial load on columns affects their shear behavior by changing the magnitude and distribution of strains, stresses, and the concrete crack inclination. In this study, the effect of axial load is considered in conjunction with the other sectional forces (bending moment and shear force) by modifying the equilibrium and compatibility equations used for the development of the beam shear hinge model. This enables accounting for the axial-flexural-shear interaction effects, which is critical for accurate prediction of the shear behavior in RC columns. The second difference is the confinement effect in RC columns due to the lateral pressure produced by the transverse reinforcement. Although the confinement effect in columns can have a substantial impact on the flexural and axial response,[10,11] its influence on the diagonal tension failure, which is the typical failure mode in shear, is negligible. This is because shear

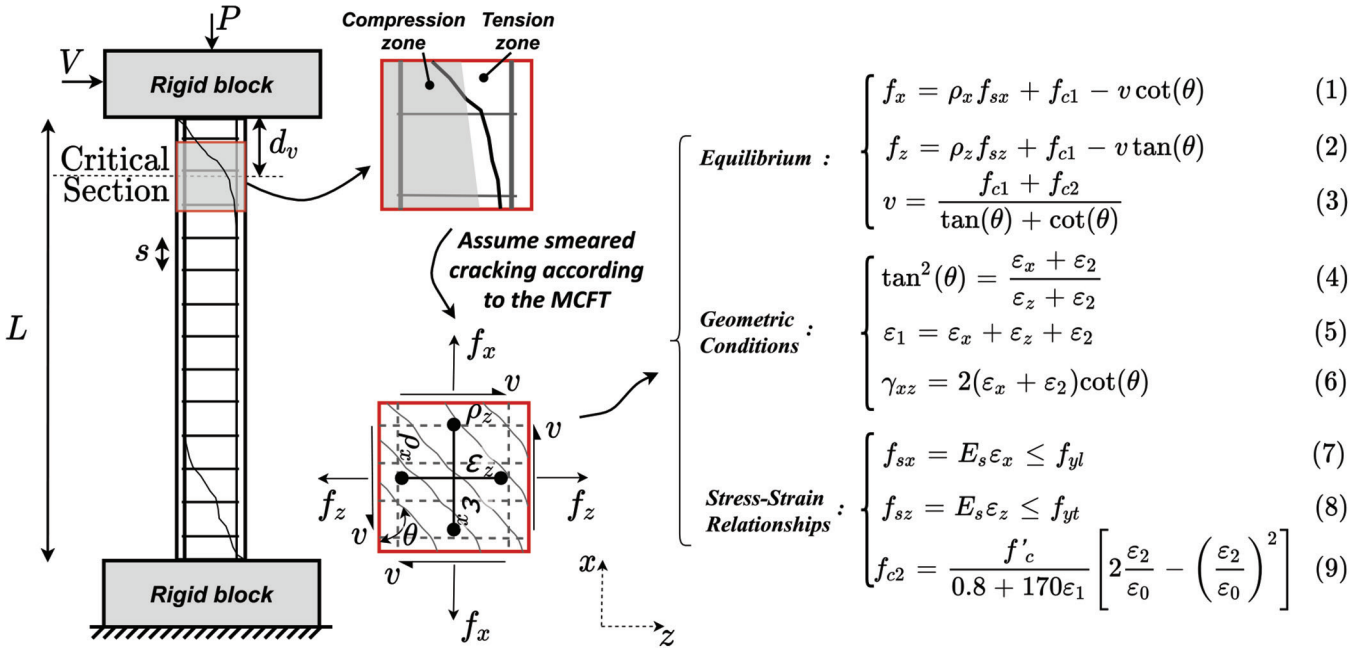

Fig. 2—Estimating shear behavior of RC column in concentrated form with 2-D panel element formulated based on MCFT.

cracks in columns are typically initiated as vertical cracks along the tension reinforcement and then extend toward the compression reinforcement as diagonal cracks. The parts of the cross section that are mostly affected by shear cracks are often under high tensile strains and therefore confinement has not much of an influence on their behavior. Confinement mainly affects the behavior in the compression zone of the column, which can be critical for the axial and flexural response because concrete crushing may take place in this zone. In this study, the confinement effect is considered in defining the concrete material properties of frame elements used to capture axial and flexural effects in columns.

As shown in Fig. 2, and similar to the procedure considered for beams, a 2-D panel element is considered at the critical section of the column to represent the nonlinear shear behavior in a concentrated form. The critical section is defined d_v (that is, effective shear depth) away from the section having maximum shear force, which is approximately the location of diagonal shear cracks observed in experimental tests and is consistent with the shear-critical section defined in the Canadian Concrete Design Code.[12] In cases where the shear force is constant throughout the column length (for example, cantilever columns), the critical section is d_v away from the section having the largest bending moment. This is because as the bending moment increases, the longitudinal strain increases, which reduces the ability of concrete to carry shear forces, resulting in a lower shear strength for the cross section.[12,13]

By evaluating the stresses and strains on the 2-D panel and using the original MCFT formulation, closed-form equations are derived to calculate the shear force and shear strain of each key point of the shear response demonstrated in Fig. 1. The original MCFT formulations, which are based on the equilibrium and compatibility conditions and stress-strain relationships, are shown in Fig. 2. The development of closed-form equations requires estimating stresses, strains, and crack inclination at the critical section of the column. By analyzing a wide range of column cross sections using the Response-2000 sectional analysis software[14] and VecTor2 FE program,[15] the nonlinear distribution of longitudinal strain (ε_x), shear strain (γ), and crack inclination (θ) along the section height is determined. Figure 3 shows an example of the nonlinear distribution of each parameter at different stages of the structural response. As it can be seen in this figure, the average value of the nonlinear distribution of each parameter is estimated using the equivalent area approach and then used for the development of closed-form equations. Unlike the original MCFT model, which is complicated and requires a trial-and-error procedure, the closed-form equations enable direct calculation of shear response, allowing the application of MCFT to the lumped plasticity analysis. Details of the closed-form equations developed for each key point of the shear response are discussed as follows. The similarities and differences between the equations proposed for columns and those previously developed for beams are highlighted.

It should be noted that the proposed shear hinge model follows a macro-modeling analysis approach and does not account for the effect of hook detailing in the reinforcement. It assumes the hook is sufficient in terms of length and bend angle and meets typical design code requirements. Also, similar to the MCFT model, the proposed shear hinge accounts for the tension-stiffening effect in the stress-strain relationship of concrete rather than altering the stress-strain response of plain steel. An alternative method to consider this effect is to use embedded bar models as proposed by Gil-Martín et al.[16,17] Unlike the MCFT model, which accounts for local stresses in the reinforcement at the crack location, the proposed model uses average reinforcement stresses in the formulation for simplicity.

Ultimate point

Similar to the beam model, the shear strength (V_u) of columns is calculated based on the Canadian Concrete

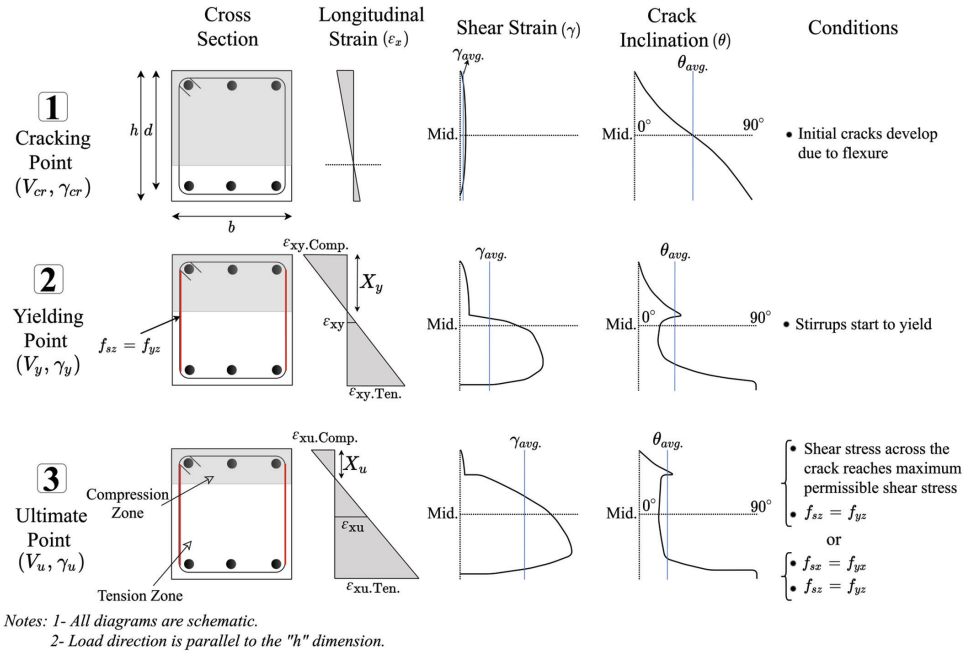

Fig. 3—Variations of longitudinal and shear strains and crack direction through section at first three key points of response.

Design Code, CSA A23.3,[12] with a few modifications. Equation (10) shows the relationship provided in the Code for computing the shear strength of an RC section which includes the contributions of both the concrete and the transverse reinforcement (V_c and V_s, respectively)

$$V_u = V_c + V_s = \beta\sqrt{f_c'}bd_v + \frac{A_{st}f_{yt}d_v}{s}\cot(\theta_u) \qquad (10)$$

where θ_u and β are the crack inclination at the ultimate shear stress and the contribution factor accounting for the strength of cracked concrete, respectively. Both parameters are a function of the longitudinal strain at midheight of the section (ε_{xu}), which can be calculated based on sectional forces (bending moment, shear force, and axial load) using Eq. (11).[13] This equation is simplified by defining two factors (k_1 and k_1'), which account for the effects of bending moment (M) and axial load (P) and will also be used in the rest of the equations presented in this study. All the k factors defined in this study are provided in the Appendix.

$$\varepsilon_{xu} = \frac{(1+\alpha)V_u + 0.5P}{2A_{sl}E_s} = \left|\frac{k_1V_u + k_1'}{1500}\right| \qquad (11)$$

In Eq. (11), α is the ratio of the bending moment to the shear force multiplied by the effective shear depth ($M/V.d_v$). Once ε_{xu} is calculated based on the sectional forces, θ_u can be found using Eq. (12). This equation was originally proposed for the beam model[3] to improve the crack inclination relationship of the CSA A23.3 design code by adding the k_6 factor in the equation to account for the effects of the yielding stress of the shear reinforcement (f_{yt}) and the compressive strength of concrete (f_c') on θ_u.

$$\theta_u = (29 + 7000\varepsilon_{xu}).(k_6) \qquad (12)$$

Figure 4 shows that this equation is also valid for columns. In this figure, the average value of the crack inclination angle along the cross section of 12 shear-critical columns obtained from the VecTor2 nonlinear FE analysis software[15] is compared against the angle computed from Eq. (12). Over the last 30 years, VecTor2 has been extensively verified against experimental data of various shear-critical structural components[18] and therefore can be considered as a reliable FE analysis tool for evaluating the performance of the proposed shear hinge model. It can be seen from Fig. 4 that the average θ_u values correlate well, demonstrating the validity of the proposed equation for the calculation of θ_u of RC columns. Structural details of the RC columns considered in this study are summarized in Table 1.

By substituting Eq. (11) into Eq. (12) and Eq. (12) into Eq. (10) and following the same procedure as that described for the beam model, the shear strength of the column cross section can be derived solely as a function of material properties and section dimensions as expressed in Eq. (13). In this equation, setting the axial load factor (k_1') to zero results in the shear strength equation previously proposed for the beam model.

$$V_u = \frac{k_1k_3 - k_4(1+k_1')}{2k_1k_4} + \sqrt{\left(\frac{k_1k_3 - k_4(1+k_1')}{2k_1k_4}\right)^2 + \frac{k_2 + k_3(1+k_1')}{k_1k_4}} \qquad (13)$$

Esfandiari and Adebar[19] showed that yielding of the longitudinal reinforcement can limit the shear strength of RC members. Based on their work, the authors proposed Eq. (14) to calculate the shear strength of beams with a low amount of flexural reinforcement[3]

$$V_u = \sqrt{(\alpha k_{15})^2 + 2k_{15}A_{sl}f_{yl}} - \alpha k_{15} \qquad (14)$$

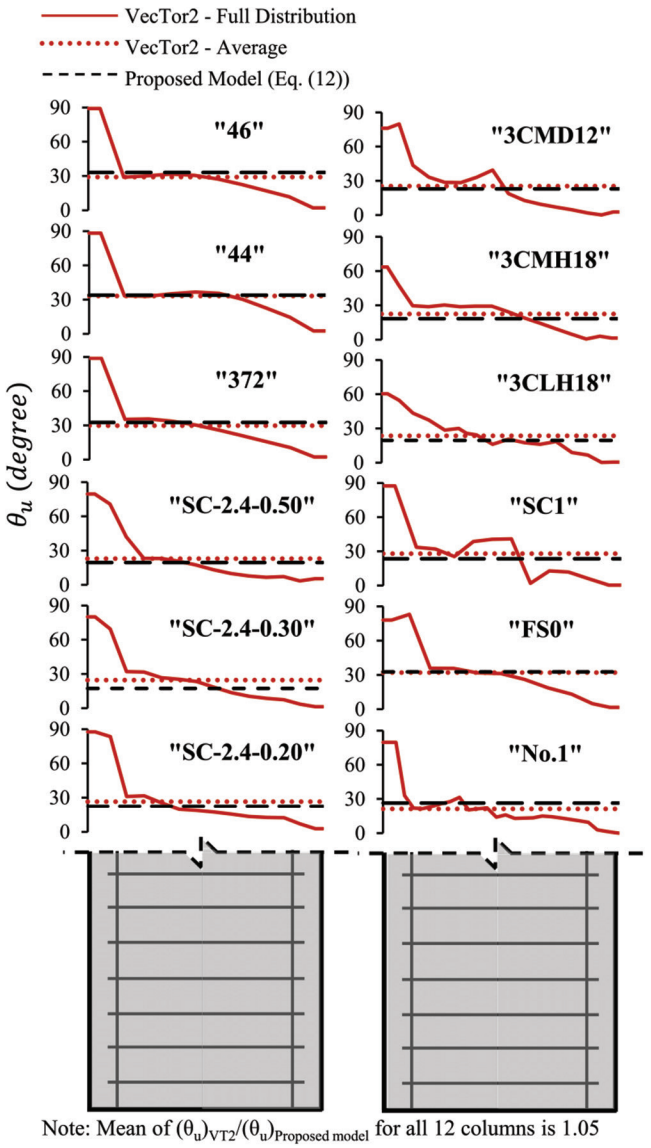

Fig. 4—Comparison of average crack inclination angle along cross section for 12 shear-critical RC columns computed by VecTor2 and proposed model.

Application of this equation to RC columns requires two modifications. First, the contribution of concrete to the shear strength was neglected in Eq. (14) and needs to be considered for columns. As previously discussed, the tension zone in columns is typically smaller than that in beams due to the axial load effect; therefore, there is more contribution from the concrete to the shear strength in columns. In this study, the concrete contribution is considered by adding the $\beta\sqrt{f_c'}bd_v$ term to Eq. (14). To be on the conservative side, the β factor is taken as 0.05, which is the minimum value recommended by CSA A23.3.[12] The second modification is to include the effect of axial load, in addition to the shear force and bending moment, in the derivation of Eq. (14). As a result of these two modifications, the following equation is proposed for the calculation of shear strength in RC columns with a low amount of flexural reinforcement

$$V_u = \sqrt{(\alpha k_{15})^2 + 2k_{15}A_{sl}f_{yl} - k_{15}P} - \alpha k_{15} + 0.05\sqrt{f_c'}bd_v \quad (15)$$

The minimum value of Eq. (13) and (15) is taken as the shear strength of RC column sections for the lumped plasticity analysis.

The shear strain at the ultimate point (γ_u) can be found from Eq. (16), which is derived by modifying Eq. (6) of the original MCFT method (refer to Fig. 2) to account for the effective shear strain depth in the section as discussed for the beam model.[3] Because Eq. (16) is determined solely based on the compatibility and strain transformation relationships, it can be used for columns as well.

$$\gamma_u = 2(\varepsilon_{xu} + \varepsilon_{2u}) \cdot \cot(\theta_u) \cdot k_9 \quad (16)$$

In Eq. (16), ε_{xu} is the longitudinal strain at the middepth of the section; ε_{2u} is the average principal compressive strain of the section; θ_u is the average crack inclination angle; and k_9 is a modification factor to account for the shear strain distribution over the depth. All these parameters are calculated at the peak shear stress (that is, the ultimate point) and are

Table 1—Parameters of RC columns considered for verification study

Researcher	Column	f_c', MPa	f_{yl}, MPa	f_{yt}, MPa	b, mm	h, mm	d, mm	a, mm	s, mm	A_{sl}, mm^2	A_{st}, mm^2	$P/f_c'A_g$	BC
Tran[24]	SC-2.4-0.20	22.6	408.0	392.6	350	350	309	850	125	2513	56.5	0.200	DC
	SC-2.4-0.30	49.3	409.0	392.6	350	350	306	850	125	3927	56.5	0.300	DC
	SC-2.4-0.50	24.2	408.0	392.6	350	350	309	850	125	2513	56.5	0.500	DC
Kokusho[25]	372	19.9	524.0	351.6	200	200	170	500	100	532	68.4	0.197	C
Lynn[26]	3CLH18	26.9	331.0	399.9	457	457	394	1473	457	6334	143.2	0.089	DC
	3CMH18	27.6	331.0	399.9	457	457	394	1473	457	6334	143.2	0.262	DC
	3CMD12	27.6	331.0	399.9	457	457	394	1473	305	6334	244.4	0.262	DC
Imai and Yamamoto[27]	No. 1	27.1	318.0	336.0	400	500	443	825	100	5322	127.2	0.072	C
Yoshimura and Yamanaka[28]	FS0	27.0	387.0	355.0	300	300	255	900	75	3438	138.6	0.260	C
Zimos et al.[29]	SC_1	32.8	565.0	565.0	300	300	254	832	320	2413	100.5	0.061	C
Ikeda[30]	44	19.6	434.0	558.0	200	200	173	500	100	796	58.4	0.100	C
	46	19.6	434.0	558.0	200	200	173	500	100	796	58.4	0.200	C

Note: "BC," "DC," and "C" stand for the Boundary Condition, Double Curvature, and Cantilever, respectively; 1 mm = 0.0394 in.; 1 MPa = 0.1450 ksi.

affected by the axial load in columns. ε_{xu} can be calculated from Eq. (17), which is similar to the equation used for the beam model developed based on the equilibrium requirements. The main difference in the calculation of ε_{xu} is the addition of the k_1' factor to the equation to account for the effect of axial load. In addition, a lower bound is considered to ensure that the value of ε_{xu} would not fall below the limit of longitudinal strain under pure axial load condition.

$$\varepsilon_{xu} = \frac{k_1 V_u + k_1'}{750} \cdot k_5 \geq \frac{P}{bh\left(0.5E_c + \rho_x E_s\right)} \tag{17}$$

In Eq. (17), the k_5 factor is a function of the compression zone depth in the section (X_u), which can be calculated using Eq. (18) developed based on the equilibrium of compression and tension forces in the section with the consideration of axial load

$$X_u = \frac{\sqrt{C\varepsilon_0\left[bdf_c'\varepsilon_{xu.Ten.} + \frac{C\varepsilon_0}{2}\right]} - \frac{C}{2}}{bf_c'\varepsilon_{xu.Ten.}} \tag{18}$$

$$C = T - P = \min\left\{(1+\alpha)V_u + 0.5P, A_{sl}f_{yl}\right\} - P \tag{19}$$

where C and T are the summation of the forces acting on the compression and tension sides of the neutral axis, respectively; and P is the applied compressive axial load, which should be considered with a negative sign. A more accurate and complicated version of Eq. (18) that considers the effect of longitudinal compression reinforcement is provided in the Appendix. In Eq. (18), $\varepsilon_{xu.Ten.}$ is the strain of the tension reinforcement at the peak shear stress, which can be computed using Eq. (20) developed by Bentz and Collins.[20]

$$\varepsilon_{xu.Ten.} = \frac{k_1 V_u + k_1'}{750} \tag{20}$$

The second variable in Eq. (16) is ε_{2u}, which can be calculated by finding the principal compressive stress in the concrete (f_{c2u}). Using Eq. (3) of the original MCFT method and neglecting the principal tensile stress in the concrete (f_{c1u}) because of high tensile strains at this stage of the response, f_{c2u} can be expressed as

$$f_{c2u} = v_u\left(\tan\theta_u + \cot\theta_u\right) \tag{21}$$

For the beam model, f_{c2u} and θ_u in Eq. (21) represented the average values of concrete stress and crack angle for the entire cross section. While this approach works well for beams, its application to columns requires some modifications. Because of the axial load, the compression depth of the section in columns is considerably larger than that in beams. To consider the contribution of the stresses in the compression zone to the average f_{c2u} of the section more accurately, instead of applying Eq. (21) to the entire cross section, f_{c2u} values of the compression and tension zones of the section are calculated separately using Eq. (22a) and (22b). The weighted average technique is then used to compute the average f_{c2u} of the section, as expressed in Eq. (23)

$$f_{c2u.Ten.} = v_u\left(\tan\theta_{u.Ten.} + \cot\theta_{u.Ten.}\right) \tag{22a}$$

$$f_{c2u.Comp.} = v_u\left(\tan\theta_{u.Comp.} + \cot\theta_{u.Comp.}\right) \tag{22b}$$

$$f_{c2u} = \frac{f_{c2u.Comp.}X_u + f_{c2u.Ten.}\left(h - X_u\right)}{h} \tag{23}$$

where $\theta_{u.Ten.}$ and $\theta_{u.Comp.}$ are the average crack inclination angle in the tension and compression zones of the section, respectively. The distribution of f_{c2u} and θ_u along the section height obtained from the VecTor2 model as well as the average values for the tension and compression zones estimated by the proposed lumped plasticity model are shown in Fig. 5. To determine $\theta_{u.Ten.}$ and $\theta_{u.Comp.}$, the distribution of the crack angle along the section is simplified into a constant and a parabolic distribution for the tension and compression zones, respectively. Using the simplified distributions and the average θ_u of the section calculated from Eq. (12), $\theta_{u.Ten.}$ and $\theta_{u.Comp.}$ can be estimated from Eq. (24).

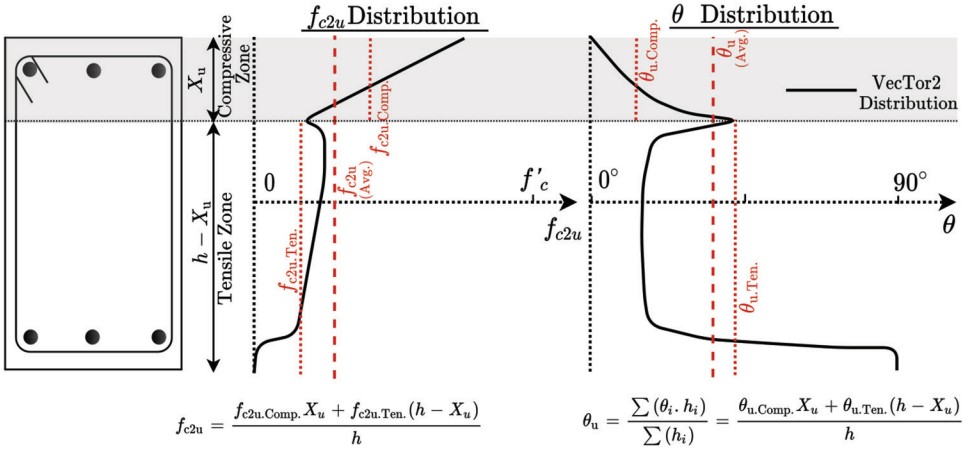

Fig. 5—Variation of principal compressive stress and crack direction through section at ultimate point.

$$\theta_{u.Ten.} = \frac{\theta_u}{1 - \frac{2X_u}{3h}} \tag{24a}$$

$$\theta_{u.Comp.} = \frac{\theta_{u.Ten.}}{3} \tag{24b}$$

By equating Eq. (23) to Eq. (9) of the original MCFT method, which represents the compressive stress-strain response of concrete based on the Hognestad model[21] while accounting for the compression softening effect (refer to Fig. 2), Eq. (25) can be derived for calculation of the principal compressive strain in concrete (ε_{2u}).

$$\varepsilon_{2u} = \max\left\{k_8, 1 - \sqrt{1 - f_{c2u}/f_c'}\right\} \times \varepsilon_0 \tag{25}$$

The overall concept for calculating ε_{2u} is the same for both the beam and column models. The only difference between the two models is in the consideration of the compression softening effect. As the axial compressive load increases in a column section, the principal tensile strain in concrete (ε_1) reduces, and as a result the reduction factor for the compression softening effect that is equal to $1/(0.8 + 170\varepsilon_1)$ (refer to Eq. (9)) may become greater than 1.0, which is not correct. Therefore, the maximum reduction factor for the compression softening effect is limited to 1.0, which occurs when the principal tensile strain in concrete is extremely low and the compression softening effect is negligible. This limit is included in the derivation of Eq. (25).

Yielding point

The shear force corresponding to the yielding of the transverse reinforcement (V_y) can be found using Eq. (26), which is derived from Eq. (2) of the original MCFT method as described in the beam model.[3]

$$V_y = \frac{\rho_z f_{yt} + f_{c1y}}{\tan\theta_y} \cdot b \cdot d_v \tag{26}$$

In Eq. (26), the effect of axial load is considered in the calculation of the principal tensile stress in concrete (f_{c1y}), which is estimated from the principal tensile strain (ε_{1y}). From Eq. (5) of the original MCFT shown in Fig. 2, ε_{1y} equals the summation of the yielding strain of stirrups (ε_{zy}), the longitudinal strain at the yielding point (ε_{xy}), and the principal compressive strain in concrete at the yielding point (ε_{2y}). Considering that ε_{zy} is typically approximately 0.002 and is relatively greater than ε_{xy} and ε_{2y} at this stage of the response,[3] f_{c1y} can be estimated as $0.2f_t'$ (20% of the concrete tensile strength) based on the tension-stiffening model of Tamai et al.[22] According to the authors' previous study,[3] this approach works well for beams where the compression depth of the section (X_u) is relatively small compared to the tension zone. However, the compression depth of the section in columns is generally much larger than that in beams because of the axial load effect, and therefore the contribution of ε_{2y} and ε_{1y} becomes more significant in comparison with ε_{zy}. This effect is taken into account in the calculation of f_{c1y} by including the ratio

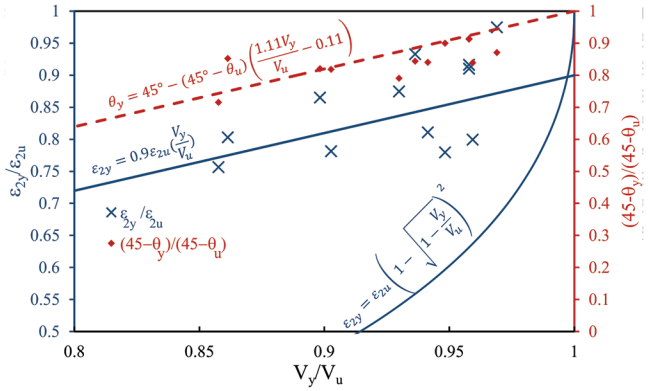

Fig. 6—Relationship between principal compressive strain in concrete, crack direction, and shear strength at yielding point and ultimate point of response.

of the compression depth to the total height of the column section (X_u/h), as can be seen in Eq. (27).

$$f_{c1y} = \left(0.2 + 0.3\frac{X_u}{h}\right) f_t' \tag{27}$$

The next parameter that needs to be calculated in Eq. (26) is θ_y. For the beam model, the authors[3] showed that there is a linear relationship between the crack angle and shear strength at the yielding point (θ_y and V_y) and those calculated at the ultimate point (θ_u and V_u). In this study, the application of this linear relationship, which is expressed in Eq. (28), to RC columns is evaluated by computing the crack angle and shear strength of 12 shear-critical columns that were previously mentioned in the "Ultimate Point" section using the VecTor2 FE analysis software. It can be seen from Fig. 6 that the FE analysis results correlate well with the predictions of Eq. (28), demonstrating that this equation is applicable to columns as well.

$$\theta_y = 45° - (45° - \theta_u)\left(\frac{1.11V_y}{V_u} - 0.11\right) \tag{28}$$

Substituting Eq. (28) into Eq. (26), the following equation can be derived for V_y

$$V_y = \begin{cases} \left|\frac{k_{11}}{2k_{12}}\right|; k_{10}k_{12} > \left(\frac{k_{11}}{2}\right)^2, \theta_u \neq 45 \\ \frac{\frac{k_{11}}{2} - \sqrt{\left(\frac{k_{11}}{2}\right)^2 - k_{10}k_{12}}}{k_{12}}; k_{10}k_{12} \leq \left(\frac{k_{11}}{2}\right)^2, \theta_u \neq 45 \leq V_u \\ k_{10}; \theta_u = 45 \end{cases} \tag{29}$$

The shear strain at the yielding point (γ_y) can be calculated with a similar approach to that described for the shear strain at the peak point (γ_u)

$$\frac{V_y}{Gbd_v} \le \gamma_y = 2\left(\varepsilon_{xy} + \varepsilon_{2y}\right)\cot\left(\theta_y\right)k_{13} \le \gamma_u \quad (30)$$

where ε_{xy} is the longitudinal strain at the middepth of the cross section; and ε_{2y} is the principal compressive strain in the concrete, both calculated at the yielding point. Similar to the procedure used for beams,[3] ε_{xy} can be calculated as the average of longitudinal strain at the outermost tensile and compressive fibers of the section ($\varepsilon_{xy.Ten.}$ and $\varepsilon_{xy.Comp.}$), as shown in Eq. (31)

$$\frac{P}{bh\left(0.5E_c + \rho_x E_s\right)} \le \varepsilon_{xy} = \frac{\varepsilon_{xy.Ten.} - \varepsilon_{xy.Comp.}}{2} \le \varepsilon_{xu} \quad (31)$$

$\varepsilon_{xy.Comp.}$ is approximately equal to the longitudinal strain in the outermost compressive fiber of the section at the peak point ($\varepsilon_{xu.Comp.}$).[3] Therefore, similar to the procedure used at the peak point, $\varepsilon_{xy.Comp.}$ can be computed using Eq. (32). $\varepsilon_{xy.Ten.}$ can also be determined from Eq. (33), which is exactly the same as Eq. (20) used for the peak point, except that V_u is replaced by V_y.

$$\varepsilon_{xyComp} = \frac{k_1 V_u + k_1'}{750} \cdot \frac{X_u}{d - X_u} \quad (32)$$

$$\varepsilon_{xy.Ten.} = \frac{k_1 V_y + k_1'}{750} \quad (33)$$

To calculate ε_{2y} in Eq. (30), a linear relationship between the principal compressive strain in the concrete and the shear force calculated at the yielding point and the peak point of the response is derived. This relationship, which is expressed in Eq. (34) and shown in Fig. 6, is found by regression analysis of data obtained from FE analysis of the aforementioned 12 RC column specimens with VecTor2. In Fig. 6, in addition to the linear relationship derived for columns, the results of a parabolic relationship previously found for beams[3] are also shown. It can be seen that the data points calculated by VecTor2 for columns correlate better with the linear equation.

$$\varepsilon_{2y} = 0.9\varepsilon_{2u} \cdot \left(\frac{V_y}{V_u}\right) \quad (34)$$

Finally, the parameter k_{13} in Eq. (30) is defined to account for the effective shear strain depth as previously described for the k_9 factor used in Eq. (16) for the ultimate point.

Cracking point

The cracking point is when initial flexural cracks develop in a section prior to the development of the shear crack. Flexural cracks develop when the longitudinal stress due to the bending moment and axial load in the section (M/S-P/A) reaches the concrete tensile strength (f_t'). Using the relationship between stresses and the parameter $\alpha = M/V.d_v$, which relates the bending moment to the shear force, Eq. (35) can be derived for the shear force at the cracking point. Setting $P = 0$ in this equation leads to the formula previously developed for the beam model.[3]

$$V_{cr} = \frac{0.33\sqrt{f_c'}bh^2 - Ph}{6\alpha d_v} \quad (35)$$

The shear strain at the cracking point (γ_{cr}) can simply be calculated by dividing the shear force by the initial shear stiffness (G)

$$\gamma_{cr} = \frac{V_{cr}}{Gbd_v} \quad (36)$$

Failure point

The post-peak response of shear-critical RC columns can be assumed to be linear with the ultimate shear strain (γ_f) occurring at the zero shear force as recommended by Elwood et al.[23] γ_f can be calculated from Eq. (37) proposed by Elwood and Moehle[8] based on a shear-friction model

$$\gamma_f = 0.04\frac{1 + \cot^2\theta_f}{\cot(\theta_f)\left(1 - P\frac{s}{A_{st}f_{yt}d_v\cot(\theta_f)}\right)}\frac{a}{2h} \quad (37)$$

where θ_f is the crack inclination angle at the failure point, which is suggested to be taken as 30 degrees for columns with axial load ratios less than 20%, and 25 degrees for columns with higher axial load ratios. As the axial compressive load increases, the longitudinal strain reduces, which leads to a lower crack inclination angle.

Figure 7 summarizes all the aforementioned equations into a four-step procedure for the calculation of the shear force and shear strain at key points of the proposed plastic hinge model.

VERIFICATION AGAINST EXPERIMENTAL TEST RESULTS

The performance and accuracy of the proposed model were assessed by comparing the results of 12 shear-critical RC columns experimentally tested by Tran,[24] Kokusho,[25] Lynn,[26] Imai and Yamamoto,[27] Yoshimura and Yamanaka,[28] Zimos et al.,[29] and Ikeda.[30] The key characteristics of the columns, including dimensions, material properties, reinforcing bar area, axial load, and boundary conditions, are shown in Table 1. While there are many other experimental studies on RC columns available in the literature,[31-33] the columns were selected from test programs with different sets of design parameters, allowing thorough performance assessment of the proposed model. Shear behavior played a significant role in the response of all the selected columns.

The OpenSees software[34] was used to model the columns with two-noded frame type elements. The nonlinear axial and flexural behavior of the columns was considered through a series of fibers defined along the cross section. To consider the confinement effect in fiber sections, the stress-strain relationship of concrete was defined according to the model of Saatcioglu and Razvi.[10] Because frame elements with fiber sections cannot account for the shear effects in RC members, a ZeroLength element with a multilinear uniaxial material behavior was added to each shear span of the columns, as shown in Fig. 1. The multilinear response of the uniaxial

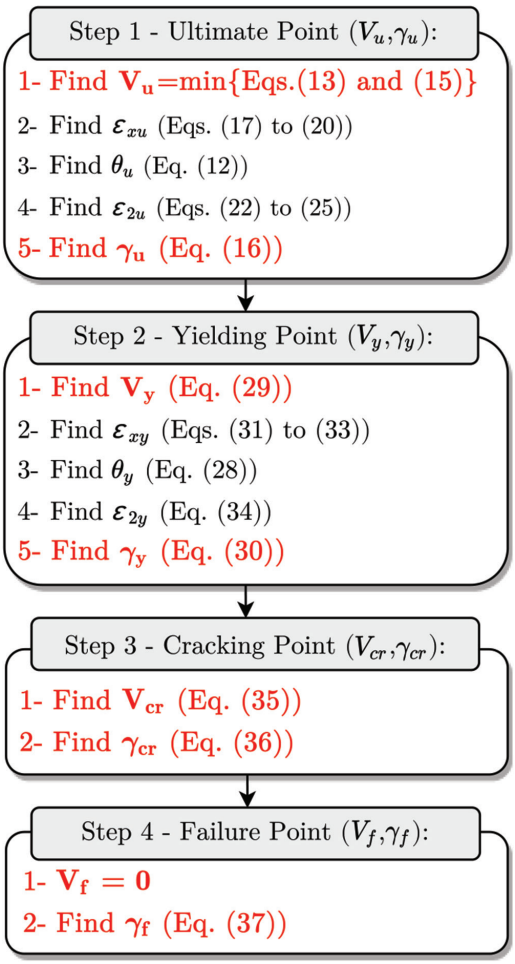

Fig. 7—Step-by-step procedure for calculation of four key points for proposed model.

material model assigned to the zero-length elements was defined based on the shear force and shear deformation values computed by the proposed plastic hinge model according to the equations presented in the previous section. The shear deformation was computed by multiplying the shear strain by the shear plastic hinge length, which can be estimated as the length of the projection of the shear crack along the longitudinal axis of the member ($d_v\cot(\theta)$).[35] Knowing that the crack inclination angle in columns ranges between 15 and 35 degrees, the plastic hinge length can be approximated as twice the section height ($2h$).

In Fig. 8, the lateral force-displacement responses of the columns computed by the OpenSees model with the proposed shear hinge elements were compared against the results of experimental tests and VecTor2. It can be seen that the force-displacement results of the OpenSees model that included the shear hinge model were in good agreement with the experimental results in terms of stiffness, peak strength, and displacement. The proposed modeling approach provided the same level of accuracy as the VecTor2 nonlinear FE analysis software with much less modeling and computing effort. Therefore, it can be regarded as a promising analysis approach for shear-critical RC structures. To demonstrate the consequences of neglecting the shear effects, the results of the OpenSees model without including shear hinge elements are also shown in Fig. 8. As expected, neglecting the shear behavior resulted in significant overestimation of strength and ductility for the shear-critical columns. Because the frame elements with fiber sections cannot capture shear failure, the analysis continued until the fibers failed due to flexural and axial load effects, resulting in highly unsafe results.

PARAMETRIC STUDY

To further verify the accuracy of the proposed shear hinge model and evaluate its application range, a comprehensive parametric study was conducted by modeling and analysis of 48 shear-critical cantilever RC columns. The VecTor2 FE analysis software was used to assess the performance of the proposed shear hinge model under various geometrical, material, and loading conditions. The selected columns varied in terms of six key design parameters—namely, the cylindrical compressive strength of concrete (f_c'), the ratio of the applied axial load to the axial capacity of the concrete section ($P/f_c'A_g$), the transverse reinforcement ratio (ρ_z), the ratio of the shear span to the section effective depth (a/d), cross-section dimensions (b or h), and the aspect ratio of the cross section (b/h). The total area of longitudinal reinforcement and the yield strength of all reinforcement are assumed to be 4200 mm^2 (6.51 in.^{2}) and 400 MPa (58.02 ksi), respectively. Other characteristics of the columns are shown in Table 2.

The characteristics of the load-deflection responses of the aforementioned columns were evaluated by determining five performance indicators for each response: 1) shear strength (V_u); 2) displacement corresponding to the peak strength (Δ_u); 3) shear force at the yielding of the transverse reinforcement (V_y); 4) area under the pre-peak portion of the response ($A_{pre\text{-}peak}$); and 5) total area under the load-deflection response (A_{total}). For each performance indicator, the ratio between the prediction of the proposed lumped plasticity analysis approach and the FE analysis (LP-to-FE) was computed.

To identify the application range and the limitations of the proposed lumped plasticity model, the variation of LP-to-FE ratios for the five performance indicators are presented in Fig. 9 as a function of design variables considered in the parametric study. Figure 9(a) shows the performance of the model as f_c' varies from 20 to 80 MPa (2.90 to 11.60 ksi). It can be seen that, for all values of f_c', the LP-to-FE ratios for all performance indicators were close to 1.0, meaning that the predictions of the lumped plasticity model agreed well with the FE analysis results. However, the accuracy of the model reduced as the concrete compressive strength increased above 50 MPa (7.25 ksi). This was expected because the Hognestad equation was used for the concrete compressive stress-strain relationship in the development of the proposed model, which is not an ideal constitutive material model for predicting the response of high-strength concrete members.

The effect of axial load is shown in Fig. 9(b). It can be seen that the proposed model accurately calculated almost all the performance indicators for axial load ratios ranging from 0.05 to 0.8. The only inconsistency was in the predictions of Δ_u for columns with axial load ratios between 0.4

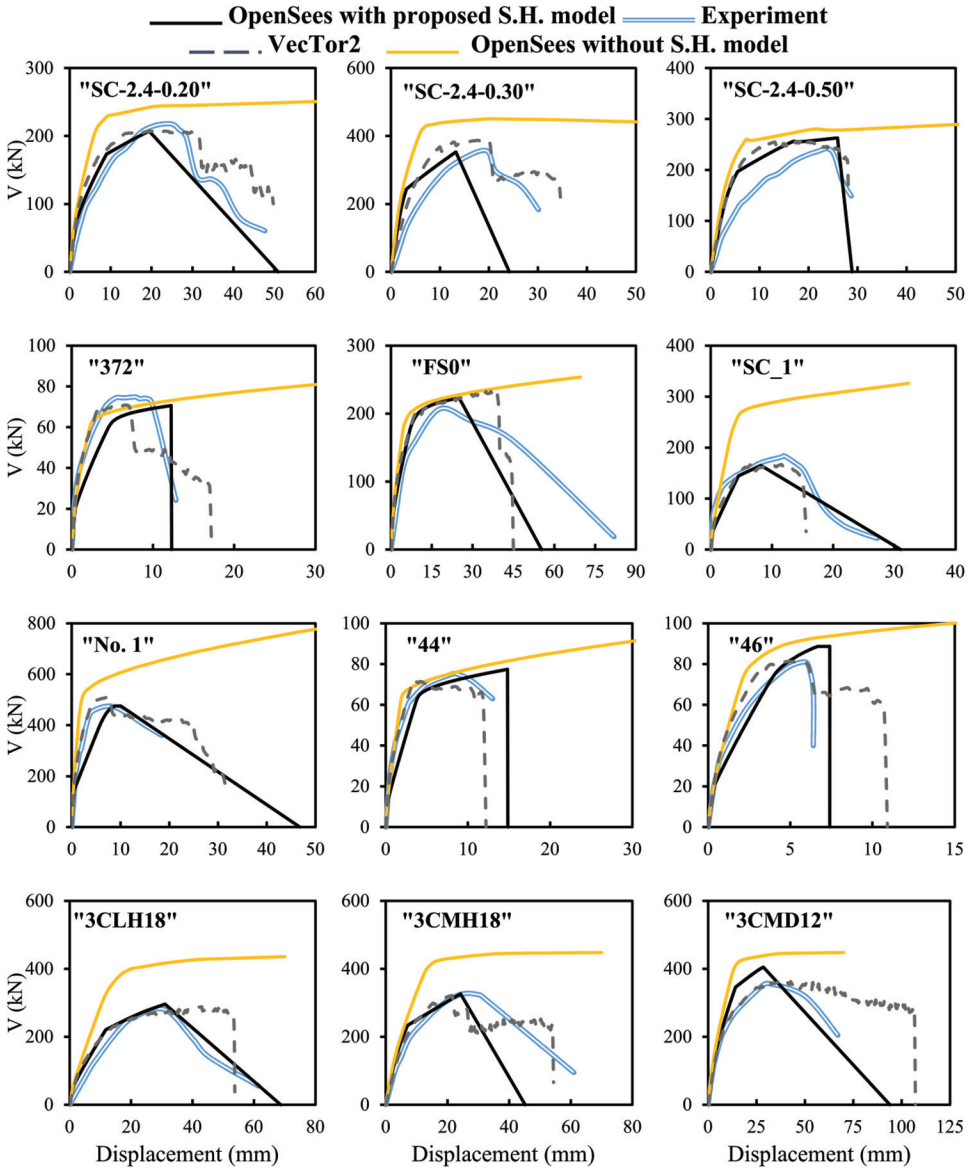

Fig. 8—Comparison of force-displacement responses between OpenSees models with and without shear hinge elements, experiment, and VecTor2. (Note: 1 mm = 0.0394 in.; 1 kN = 0.225 kip.)

and 0.6, where Δ_u was overestimated to some extent by the proposed model. Nevertheless, this did not affect the overall performance of the model for these columns, as the rest of the performance indicators, including the total area and the area under the pre-peak response, were predicted with good accuracy. From Fig. 9(c), it can be seen that the proposed model calculated the response of RC columns that contained at least the minimum amount of shear reinforcement specified according to the CSA A23.3 design code[12] reasonably well.

Figure 9(d) shows the performance of the model for shear span-depth ratios (a/d) from approximately 1 to 6. It can be seen that as the a/d reduced below 2, the accuracy of the proposed model started to deteriorate. This is because the model was developed based on the assumption that plane sections remain plane (that is, beam action) and the arch action, which occurs in deep members, was not considered in its formulation. The effect of size and the aspect ratio of the cross section were investigated in Fig. 9(e) and (f). It is shown that the proposed model was able to calculate the shear response of RC columns with cross-section sizes varying from 250 to 1500 mm (9.84 to 59.06 in.) and aspect ratios between 0.5 and 2.0 with good accuracy. For larger cross sections, the accuracy of the model was slightly lower, which could be due to the size effect in concrete.

VERIFICATION AT SYSTEM LEVEL

The effectiveness of the proposed shear hinge model for the system-level performance assessment of RC structures was evaluated by analyzing a four-story three-span frame structure representing an RC building constructed in the late 1990s in Vancouver, BC, Canada. The geometry of the frame as well as properties of member cross sections are shown in Fig. 10. The frame was designed according to the requirements of CSA A23.3-94,[36] which was the applicable design code at the time of construction. However, due to the improvements made in the Canadian design practice over the last 25 years, the frame does not meet some of the requirements of the current edition of the code (CSA A23.3:19[12]). One of the most noticeable changes in the Canadian design

Table 2—Properties of RC columns used for parametric study

Model	f_c', MPa	$P/f_c'A_g$	ρ_z, %	a/d	h, mm	b/h	Model	f_c', MPa	$P/f_c'A_g$	ρ_z, %	a/d	h, mm	b/h
C1	30	0.20	0.20	2.39	400	1.00	C25	30	0.20	0.08	2.39	400	1.00
C2	20	0.20	0.20	2.39	400	1.00	C26	30	0.20	0.07	2.39	400	1.00
C3	25	0.20	0.20	2.39	400	1.00	C27	30	0.20	0.20	1.19	400	1.00
C4	35	0.20	0.20	2.39	400	1.00	C28	30	0.20	0.20	1.49	400	1.00
C5	40	0.20	0.20	2.39	400	1.00	C29	30	0.20	0.20	1.79	400	1.00
C6	45	0.20	0.20	2.39	400	1.00	C30	30	0.20	0.20	2.09	400	1.00
C7	50	0.20	0.20	2.39	400	1.00	C31	30	0.20	0.20	2.69	400	1.00
C8	60	0.20	0.20	2.39	400	1.00	C32	30	0.20	0.20	2.99	400	1.00
C9	70	0.20	0.20	2.39	400	1.00	C33	30	0.20	0.20	3.58	400	1.00
C10	80	0.20	0.20	2.39	400	1.00	C34	30	0.20	0.20	4.48	400	1.00
C11	30	0.05	0.20	2.39	400	1.00	C35	30	0.20	0.20	5.97	400	1.00
C12	30	0.10	0.20	2.39	400	1.00	C36	30	0.20	0.20	2.39	250	1.00
C13	30	0.30	0.20	2.39	400	1.00	C37	30	0.20	0.20	2.39	300	1.00
C14	30	0.40	0.20	2.39	400	1.00	C38	30	0.20	0.20	2.39	500	1.00
C15	30	0.50	0.20	2.39	400	1.00	C39	30	0.20	0.20	2.39	600	1.00
C16	30	0.60	0.20	2.39	400	1.00	C40	30	0.20	0.20	2.39	800	1.00
C17	30	0.70	0.20	2.39	400	1.00	C41	30	0.20	0.20	2.39	1000	1.00
C18	30	0.80	0.20	2.39	400	1.00	C42	30	0.20	0.20	2.39	1200	1.00
C19	30	0.20	0.80	2.39	400	1.00	C43	30	0.20	0.20	2.39	1500	1.00
C20	30	0.20	0.40	2.39	400	1.00	C44	30	0.20	0.20	2.39	400	0.50
C21	30	0.20	0.27	2.39	400	1.00	C45	30	0.20	0.20	2.39	400	0.75
C22	30	0.20	0.16	2.39	400	1.00	C46	30	0.20	0.20	2.39	400	1.25
C23	30	0.20	0.13	2.39	400	1.00	C47	30	0.20	0.20	2.39	400	1.50
C24	30	0.20	0.10	2.39	400	1.00	C48	30	0.20	0.20	2.39	400	2.00

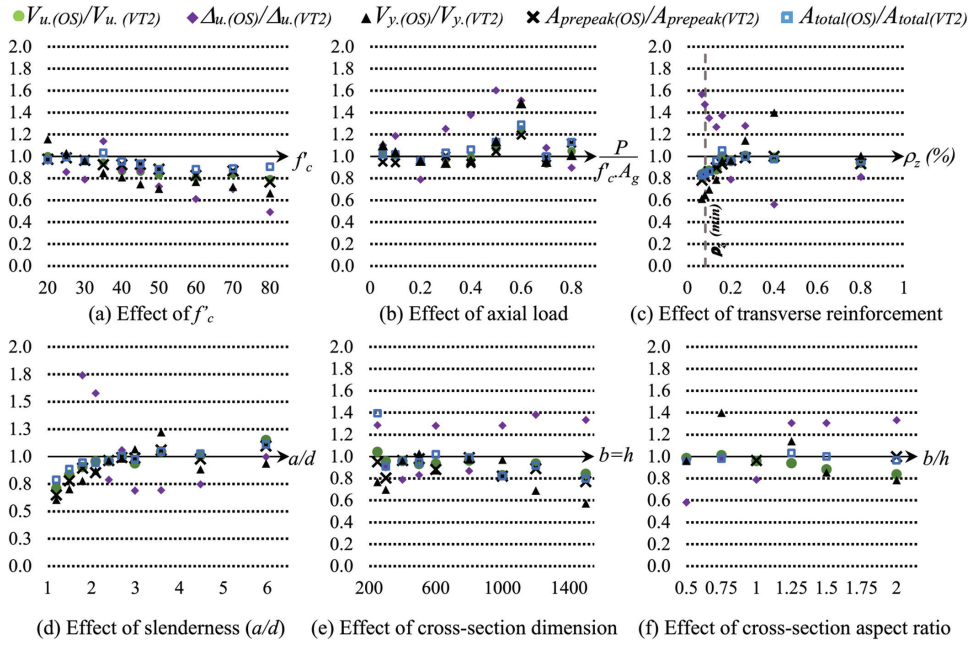

Fig. 9—Performance of proposed shear hinge model for RC columns with various design parameters. (Note: 1 mm = 0.0394 in.; 1 kN = 0.225 kip.)

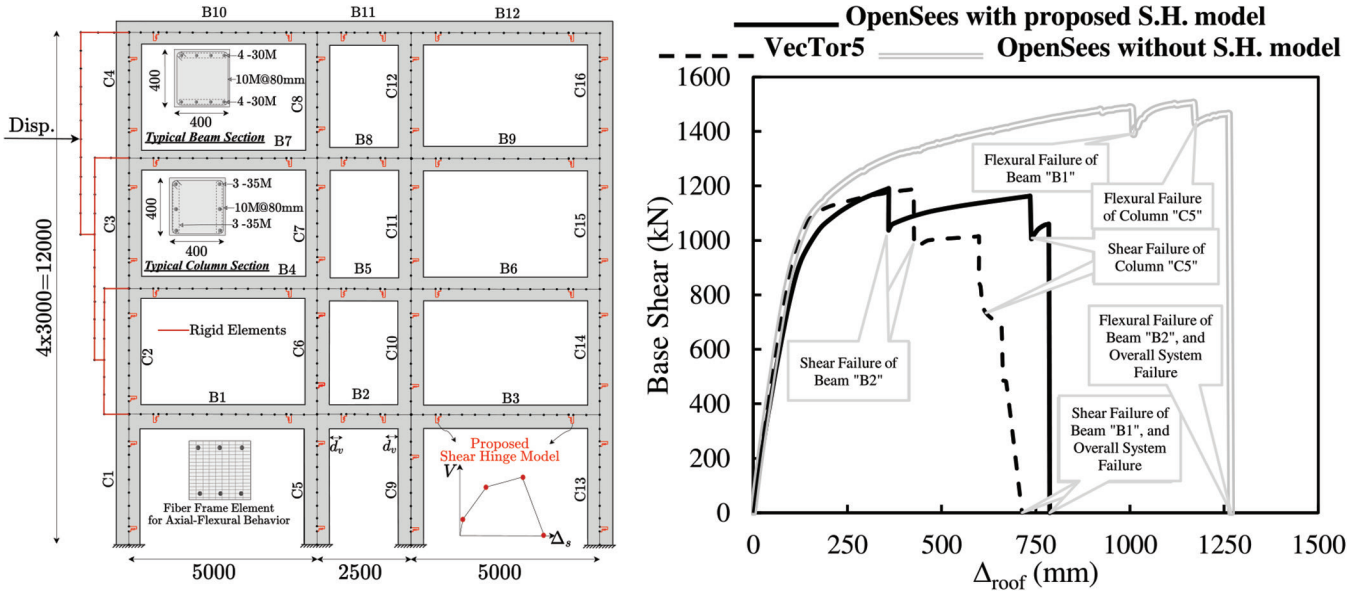

Fig. 10—System-level OpenSees model and base shear versus lateral roof displacement responses of RC frame. (Note: 1 mm = 0.0394 in.; 1 kN = 0.225 kip.)

code has been the addition of stringent requirements for volumetric transverse reinforcement in columns located in seismic regions. The lack of these requirements in the older versions of CSA A23.3 design code has raised concerns about the safety of some existing RC structures under earthquakes.

The structure was modeled using frame-type fiber-based elements in OpenSees and VecTor5[37] software. VecTor5 is a distributed plasticity analysis software for RC frames, developed based on the MCFT model.[7] Unlike most frame-type analysis software, the fiber-based elements in VecTor5 can capture nonlinearity effects due to shear in addition to the flexural and axial behavior. In the OpenSees model, the shear behavior was considered based on the lumped plasticity models presented in this paper and the previous study by the authors,[3] while the flexural and axial behavior were considered using the distributed plasticity approach with fiber-based elements. The stress-strain relationship of concrete for fiber sections was defined according to the confinement model of Saatcioglu and Razvi.[10] To consider shear effects, zero-length elements with shear hinge models were added to the ends of columns and beams of the frame, as shown in Fig. 10.

Pushover analyses were conducted on the OpenSees and VecTor5 models to simulate the seismic loads on the structure. The frame was subjected to a monotonically increasing lateral displacement applied through a series of rigid elements attached to the frame structure using simply supported connections. The location of the applied lateral load and the configuration of the rigid elements were selected such that the lateral seismic force distribution in the structure was proportional to the floor level height and the mass of each story.[38] Gravity loads (dead, live, and snow) for a typical residential building as defined in NBCC:1995[39] were also applied on the beams.

The base shear versus the lateral roof-displacement response is shown in Fig. 10 for three different analysis cases: the OpenSees analysis with and without the shear hinge models and the VecTor5 analysis. It can be seen in Fig. 10 that both the force-deflection responses and the sequence of failure obtained from VecTor5 and the OpenSees model with the shear hinges were similar. Both analysis methods predicted that the structural collapse was initiated by the shear failure of the shorter beam in the first story (B2), followed by the shear failure of the adjacent column C5 and beam B1, which then resulted in complete collapse of the structural system. As shown in Fig. 10, the OpenSees model without the shear hinges resulted in a completely different damage sequence and mode of failure along with considerable overestimation of the strength and ductility of the frame. In terms of the analysis time, the OpenSees model with the shear hinges was approximately 78% faster than the VecTor5 model, where the shear behavior was considered in a distributed manner. For larger structural systems or 3-D models, the difference between the analysis time of the two modeling methods is expected to be even higher.

SUMMARY AND CONCLUSIONS

A new lumped plasticity model was developed based on the Modified Compression Field Theory (MCFT) method to predict the response of shear-critical reinforced concrete (RC) columns. The model represents the nonlinear shear behavior of columns in a concentrated manner through a set of closed-form equations derived by simplifying the complex procedure of the original MCFT method. The model formulation takes into account the shear-flexure-axial interaction effects and complex material mechanisms in RC such as tension stiffening and compression softening. Moreover, it considers the nonlinear distribution of stresses, strains, and the crack inclination through the section height in an average sense.

The accuracy of the proposed model was verified through analysis of 12 shear-critical RC columns tested by different researchers using the OpenSees software. It was shown that the model can calculate the response of shear-critical columns reasonably well in terms of strength, ductility, and stiffness. The analysis results also indicated that neglecting

the nonlinearity effects due to shear can result in significant overestimation of the peak strength and ductility, leading to unsafe predictions. Afterward, using a comprehensive parametric study on columns with various design parameters, the application range and the limitations of the model were identified. The design parameters that were investigated included material properties, loading condition, and cross-sectional details. The model performed well for almost all RC columns, except those with a shear span to effective depth ratio of less than 2.0, which was expected as the arch action was not considered in the model formulation. Also, the accuracy of the model was reduced for high-strength concrete columns or columns with transverse reinforcement ratios less than the minimum value specified by the Canadian design code.[12] Finally, the effectiveness of the proposed model for the system-level analysis of RC structures was evaluated by modeling a multi-story frame structure with shear-critical members. The results demonstrated that the proposed lumped plasticity model can effectively consider nonlinear shear deformations and shear failure modes in RC frames with the same level of accuracy as the distributed plasticity method but with considerably less computational time.

The use of the proposed shear hinge model for columns and the previously developed model for beams will assist engineers to evaluate the safety and performance of large RC structures while considering the nonlinear shear behavior of different structural members in an accurate and practical manner. The proposed shear hinge models can be easily used with any type of frame analysis software without requiring any changes to the software formulation.

AUTHOR BIOS

Amir Reza Tabkhi Wayghan *is an MASc student at Carleton University, Ottawa, ON, Canada. He received his BSc and his first MASc in civil engineering with specialization in structural engineering from the Sharif University of Technology, Tehran, Iran. His research interests include assessment of reinforced concrete structures, strengthening of structures, and performance-based design.*

Vahid Sadeghian *is an Assistant Professor in the Department of Civil and Environmental Engineering at Carleton University. His research interests include nonlinear analysis and design of concrete structures, constitutive modeling, performance assessment and forensic investigation, and rehabilitation of structures.*

NOTATION

$A_{pre\text{-}peak}$	=	area under pre-peak portion of response
A_{sl}	=	area of tensile longitudinal reinforcement
A_{st}	=	area of transverse reinforcement
A_{total}	=	total area under load-deflection response
a	=	shear span
b	=	beam width
C	=	summation of forces acting on compression side of cross section
d	=	effective depth
d_v	=	effective shear depth, taken as greater of $0.9d$ or $0.72h$
E_s	=	modulus of elasticity of steel
f_c'	=	cylindrical compressive strength of concrete
f_{c1}	=	principal tensile stress in concrete
f_{c2}	=	principal compressive stress in concrete
f_{sx} and f_{sz}	=	average stress in longitudinal and transverse reinforcement
f_t'	=	modulus of rupture of concrete
f_x and f_z	=	stress applied to element in x- and z-directions
f_{yl}	=	yield strength of longitudinal reinforcement
f_{yt}	=	yield strength of transverse reinforcement
G	=	initial shear modulus of concrete
h	=	beam height
P	=	axial compressive load (negative sign for compression)
s	=	spacing of transverse reinforcement
s_z	=	crack spacing parameter, as defined in CSA A23.3
s_{ze}	=	equivalent crack spacing that allows for influence of aggregate size
T	=	summation of forces acting on tension side of cross section
V	=	shear force
V_c	=	shear resistance provided by concrete
V_s	=	shear resistance provided by transverse reinforcement
v	=	shear stress
v_c	=	shear stress in concrete
v_{ci}	=	shear stress on crack surfaces
X	=	distance from extreme compression fiber to neutral axis
β	=	contribution factor accounting for strength of cracked concrete
ε_x	=	longitudinal strain
ε_z	=	transverse strain
ε_0	=	strain in concrete at f_c'
ε_1	=	principal tensile strain in concrete
ε_2	=	principal compressive strain in concrete
γ	=	shear strain
θ	=	angle between crack inclination and x-axis
ρ_x and ρ_z	=	longitudinal and transverse reinforcement ratios

Note: Subscripts "*u*," "*f*," "*y*," and "*cr*" = related to each of four key points in model.

REFERENCES

1. Sadeghian, V.; Kwon, O.-S.; and Vecchio, F. J., "A Framework for Multi-Platform Simulation of RC Structures," *Engineering Structures*, V. 181, 2019, pp. 260-270. doi: 10.1016/j.engstruct.2018.12.023

2. Sadeghian, V.; Kwon, O.-S.; and Vecchio, F. J., "Modeling Beam-Membrane Interface in Reinforced Concrete Frames," *ACI Structural Journal*, V. 115, No. 3, May 2018, pp. 825-835. doi: 10.14359/51701130

3. Tabkhi, A. R., and Sadeghian, V., "A Shear Hinge Model for Analysis of Reinforced Concrete Beams," *ACI Structural Journal*, V. 118, No. 6, Nov. 2021, pp. 279-291.

4. Pincheira, J. A.; Dotiwala, F. S.; and D'Souza, J. T., "Seismic Analysis of Older Reinforced Concrete Columns," *Earthquake Spectra*, V. 15, No. 2, 1999, pp. 245-272. doi: 10.1193/1.1586040

5. Elwood, K. J., "Modelling Failures in Existing Reinforced Concrete Columns," *Canadian Journal of Civil Engineering*, V. 31, No. 5, 2004, pp. 846-859. doi: 10.1139/l04-040

6. LeBorgne, M. R., and Ghannoum, W. M., "Analytical Element for Simulating Lateral-Strength Degradation in Reinforced Concrete Columns and Other Frame Members," *Journal of Structural Engineering*, ASCE, V. 140, No. 7, 2014, p. 04014038. doi: 10.1061/(ASCE)ST.1943-541X.0000925

7. Vecchio, F. J., and Collins, M. P., "The Modified Compression-Field Theory for Reinforced Concrete Elements Subjected to Shear," *ACI Journal Proceedings*, V. 83, No. 2, Mar.-Apr. 1986, pp. 219-231.

8. Elwood, K. J., and Moehle, J. P., "Axial Capacity Model for Shear-Damaged Columns," *ACI Structural Journal*, V. 102, No. 4, July-Aug. 2005, pp. 578-587.

9. Tran, C. T. N., and Li, B., "Experimental Studies on the Backbone Curves of Reinforced Concrete Columns with Light Transverse Reinforcement," *Journal of Performance of Constructed Facilities*, ASCE, V. 29, No. 5, 2015, p. 04014126. doi: 10.1061/(ASCE)CF.1943-5509.0000626

10. Saatcioglu, M., and Razvi, S. R., "Strength and Ductility of Confined Concrete," *Journal of Structural Engineering*, ASCE, V. 118, No. 6, 1992, pp. 1590-1607. doi: 10.1061/(ASCE)0733-9445(1992)118:6(1590)

11. Dong, C. X.; Kwan, A. K. H.; and Ho, J. C. M., "A Constitutive Model for Predicting the Lateral Strain of Confined Concrete," *Engineering Structures*, V. 91, 2015, pp. 155-166. doi: 10.1016/j.engstruct.2015.02.014

12. CSA A23.3:19, "Design of Concrete Structures," CSA Group, Toronto, ON, Canada, 2019, 301 pp.

13. Bentz, E. C.; Vecchio, F. J.; and Collins, M. P., "Simplified Modified Compression Field Theory for Calculating Shear Strength of Reinforced Concrete Elements," *ACI Structural Journal*, V. 103, No. 4, July-Aug. 2006, pp. 614-624.

14. Bentz, E., and Collins, M. P., "Response-2000, Membrane-2000, Triax-2000, and Shell-2000 User Manual," 2001, https://cupdf.com/document/response-2k-user-manual-final.html.

15. Wong, P. S.; Vecchio, F. J.; and Trommels, H., "VecTor2 and FormWorks User's Manual: Second Edition," Department of Civil Engineering, University of Toronto, Toronto, ON, Canada, 2013, 318 pp.

16. Gil-Martín, L. M.; Hernández-Montes, E.; Aschheim, M. A.; and Pantazopoulou, S., "Refinements to Compression Field Theory, with Application to Wall-Type Structures," *Thomas T.C. Hsu Symposium: Shear and Torsion in Concrete Structures*, SP-265, A. Belarbi, Y. L. Mo, and A. Ayoub, eds., American Concrete Institute, Farmington Hills, MI, 2009, pp. 123-142.

17. Gil-Martín, L. M.; Hernández-Montes, E.; Aschheim, M. A.; and Pantazopoulou, S. J., "A Simpler Compression-Field Theory for Structural Concrete," *Studies and Researches - Annual Review of Structural Concrete*, V. 31, 2011, pp. 11-42.

18. Sadeghian, V., and Vecchio, F., "The Modified Compression Field Theory: Then and Now," *Shear in Structural Concrete*, SP-328, D. Mitchell and A. Belarbi, eds., American Concrete Institute, Farmington Hills, MI, 2018, pp. 3.1-3.20.

19. Esfandiari, A., and Adebar, P., "Shear Strength Evaluation of Concrete Bridge Girders," *ACI Structural Journal*, V. 106, No. 4, July-Aug. 2009, pp. 416-426.

20. Bentz, E. C., and Collins, M. P., "Development of the 2004 Canadian Standards Association (CSA) A23.3 Shear Provisions for Reinforced Concrete," *Canadian Journal of Civil Engineering*, V. 33, No. 5, 2006, pp. 521-534. doi: 10.1139/l06-005

21. Hognestad, E., "Study of Combined Bending and Axial Load in Reinforced Concrete Members," University of Illinois Engineering Experiment Station, Bulletin Series No. 399, V. 49, No. 22, 1951, 128 pp.

22. Tamai, S.; Shima, H.; Izumo, J.; and Okamura, H., "Average Stress-Strain Relationship in Post Yield Range of Steel Bar in Concrete," *Concrete Library of JSCE*, No. 11, 1988, pp. 117-129.

23. Elwood, K. J.; Matamoros, A. B.; Wallace, J. W.; Lehman, D. E.; Heintz, J. A.; Mitchell, A. D.; Moore, M. A.; Valley, M. T.; Lowes, L. N.; Comartin, C. D.; and Moehle, J. P., "Update to ASCE/SEI 41 Concrete Provisions," *Earthquake Spectra*, V. 23, No. 3, 2007, pp. 493-523. doi: 10.1193/1.2757714

24. Tran, C. T. N., "Experimental and Analytical Studies on the Seismic Behavior of Reinforced Concrete Columns with Light Transverse Reinforcement," PhD thesis, Nanyang Technological University, Singapore, 2010, 183 pp.

25. Kokusho, S., Reported by Hirosawa M., "A List of Past Experimental Results of Reinforced Concrete Columns," Report No. 2, Building Research Institute, Tsukuba, Japan, 1973, 326 pp.

26. Lynn, A. C., "Seismic Evaluation of Existing Reinforced Concrete Building Columns," PhD thesis, University of California, Berkeley, Berkeley, CA, 2001, 359 pp.

27. Imai, H., and Yamamoto, Y., "A Study on Causes of Earthquake Damage of Izumi High School Due to Miyagi-Ken-Oki Earthquake in 1978," *Transactions of the Japan Concrete Institute*, V. 8, 1986, pp. 405-418.

28. Yoshimura, M., and Yamanaka, N., "Ultimate Limit State of RC Columns," *Second U.S.-Japan Workshop on Performance-Based Earthquake Engineering Methodology for Reinforced Concrete Structures*, PEER Center, Sapporo, Hokkaido, Japan, 2000, pp. 313-326.

29. Zimos, D. K.; Papanikolaou, V. K.; Kappos, A. J.; and Mergos, P. E., "Shear-Critical Reinforced Concrete Columns under Increasing Axial Load," *ACI Structural Journal*, V. 117, No. 5, Sept. 2020, pp. 29-39.

30. Ikeda, A., *Report of the Training Institute for Engineering Teachers*, Yokohama National University, Yokohama, Kanagawa, Japan, 1968.

31. Wight, J. K., and Sozen, M. A., "Shear Strength Decay in Reinforced Concrete Columns Subjected to Large Deflection Reversals," Structural Research Series No. 403, Civil Engineering Studies, University of Illinois at Urbana-Champaign, Urbana, IL, 1973, 290 pp.

32. Aboutaha, R. S.; Engelhardt, M. D.; Jirsa, J. O.; and Kreger, M. E., "Rehabilitation of Shear Critical Concrete Columns by Use of Rectangular Steel Jackets," *ACI Structural Journal*, V. 96, No. 1, Jan.-Feb. 1999, pp. 68-78.

33. Sezen, H., and Moehle, J. P., "Seismic Behavior of Shear-Critical Reinforced Concrete Building Columns," *Seventh U.S. National Conference on Earthquake Engineering*, Boston, MA, 2002, pp. 3847-3856.

34. Mazzoni, S.; McKenna, F.; Scott, M. H.; and Fenves, G. L., "OpenSees Command Language Manual," Pacific Earthquake Engineering Research (PEER) Center, University of California, Berkeley, Berkeley, CA, 2006, 465 pp.

35. Salgado, R. A., and Guner, S., "A Comparative Study on Nonlinear Models for Performance-Based Earthquake Engineering," *Engineering Structures*, V. 172, 2018, pp. 382-391. doi: 10.1016/j.engstruct.2018.06.034

36. CSA A23.3-94, "Design of Concrete Structures," CSA Group, Toronto, ON, Canada, 1994, 199 pp.

37. Guner, S., and Vecchio, F. J., "User's Manual of VecTor5," 2008, 95 pp., http://www.vectoranalysisgroup.com/software.html.

38. Calvi, G. M.; Magenes, G.; and Pampanin, S., "Experimental Test on a Three Storey RC Frame Designed for Gravity Only," *12th European Conference on Earthquake Engineering*, London, UK, Paper No. 727, 2002.

39. Canadian Commission on Building and Fire Codes, "National Building Code of Canada: 1995," National Research Council Canada, Ottawa, ON, Canada, 1995, 571 pp.

Table A1—Appendix (equations for factors)

$k_1 = \frac{750(1+\alpha)}{A_{sl}E_s}$	$k_1' = \frac{375P}{A_{sl}E_s}$	$k_2 = 0.4\sqrt{f_c'}bd_v\frac{1300}{1000+s_{ze}}(\text{SI})$ $\left(k_2 = 4.8\sqrt{f_c'}bd_v\frac{51}{39+s_{ze}}(\text{Imperial})\right)$	
$k_3 = (1.73-0.2k_1')\xi$	$k_4 = 1+0.2\xi k_1$	$k_5 = \frac{\frac{h}{2}-X_u}{d-X_u}$	$k_7' = A_{s.Comp.}\varepsilon_{x.Ten.}E_s$
$k_6 = \begin{cases} 1.0 & ; \ \frac{\rho_z f_{yt}}{f_c'} \geq 0.1 \\ \left(\frac{\rho_z f_{yt}}{0.1f_c'}\right)^{0.2} & ; \ 0 < \frac{\rho_z f_{yt}}{f_c'} < 0.1 \end{cases}$		$k_9 = \frac{h}{d-X_u} \leq \frac{h}{h-d}$	
$k_{10} = (\rho_z f_{yt} + f_{c1y})b.d_v$	$k_8 = \mu\varepsilon_0 - 1 + \sqrt{(\mu\varepsilon_0-1)^2 + 4\mu\varepsilon_{xu}\frac{\delta}{\delta+1} + 0.8\frac{f_{c2u}}{f_c'}}$		
$k_{11} = \frac{400-\theta_u}{360}$	$k_{12} = \frac{45-\theta_u}{36.V_u}$	$k_{13} = \frac{h}{d-X_y} \leq 1.2k_9$	
$k_{15} = \frac{A_{st}f_{yt}d_v}{s}$	$\alpha = \frac{M_f}{V_f d_v} \geq 1.0$	$\delta = \sqrt{1+\tan^2(2\theta_u)}$	$\xi = \frac{\frac{A_{st}f_{yt}d_v}{s}}{\left(\frac{\rho_z f_{yt}}{0.1f_c'}\right)^{0.23}}$ $\mu = 85\frac{\delta+1}{\delta-1}\frac{f_{c2u}}{f_c'}$
$X_y = \frac{\varepsilon_{xy.Comp.}}{\varepsilon_{xy.Comp.}+\varepsilon_{xy.Ten.}}d$	$s_{ze} = \frac{35s_z}{15+a_g} \geq 0.85s_z(\text{SI})$ $\left(s_{ze} = \frac{1.38s_z}{0.59+a_g} \geq 0.85s_z(\text{Imperial})\right)$		
$X_u = \begin{cases} \frac{\sqrt{\frac{k_7'^2\varepsilon_0^2}{4} + k_7'\varepsilon_0\left[bd'f_c'\varepsilon_{xu.Ten.} + \frac{C\varepsilon_0}{2}\right] + C\varepsilon_0\left[bdf_c'\varepsilon_{xu.Ten.} + \frac{C\varepsilon_0}{2}\right]} - \frac{k_7'+C}{2}}{bf_c'\varepsilon_{xu.Ten.}} & ; \text{Advanced equation} \\ \frac{\sqrt{C\varepsilon_0\left[bdf_c'\varepsilon_{xu.Ten.} + \frac{C\varepsilon_0}{2}\right]} - \frac{C}{2}}{bf_c'\varepsilon_{xu.Ten.}} & ; \text{Simplified equation} \end{cases}$			

Note: Factors that are added/changed to/from beam model[3] are in shaded cells.